Egyptian Journal of Petroleum (2013) 22, 225–240

Egyptian Petroleum Research Institute

Egyptian Journal of Petroleum

www.elsevier.com/locate/egyjp
www.sciencedirect.com

# Carbon dioxide injection for enhanced gas recovery and storage (reservoir simulation)

Chawarwan Khan [a,*], Robert Amin [b], Gary Madden [c]

[a] Dept of Petroleum Engineering, Curtin University, Perth, Australia
[b] Clean Gas Technology Australia, Curtin University, Perth, Australia
[c] School of Economics and Finance, Curtin University, Perth, Australia

Received 7 June 2012; accepted 6 August 2012

**KEYWORDS**

$CO_2$ reinjection;
Methane recovery;
$CO_2$ sequestration;
Net carbon credit;
Economic evaluation

**Abstract** $CO_2$ injection for enhanced oil recovery (EOR) had been broadly investigated both physically and economically. The concept for enhanced gas recovery (EGR) is a new area under discussion that had not been studied as comprehensively as EOR. In this paper, the "Tempest" simulation software was used to create a three-dimensional reservoir model. The simulation studies were investigated under different case scenarios by using experimental data produced by Clean Gas Technology Australia (CGTA). The main purpose of this study is to illustrate the potential of enhanced natural gas recovery and $CO_2$ storage by re-injecting $CO_2$ production from the natural gas reservoir. The simulation results outlined what factors are favourable for the $CO_2$-EGR and storage as a function of $CO_2$ breakthrough in terms of optimal timing of $CO_2$ injection and different injection rates. After analysing the results for each case scenario, it had been concluded that $CO_2$ injection can be applied to increase natural gas recovery simultaneously sequestering a large amount of the injected $CO_2$ for this particular gas reservoir. In addition, various $CO_2$ costs involved in the $CO_2$-EGR and storage were investigated to determine whether this technique is feasible in terms of the $CO_2$ content in the production as a preparation stage to achieve the economic analysis for the model.



## 1. Introduction

$CO_2$ emissions from fossil fuel had strong impacts on the environment, and its amount in the atmosphere was far beyond to be ignored [19]. Currently there is a rising global attention to reduce carbon dioxide ($CO_2$) emissions from fossil fuels' burning. Conversely, there is a rising interest in petroleum companies to use $CO_2$ as an approach for enhanced oil or/and gas (EOR & EGR) relatively to deal with the rapid growth in world energy demands [2]. These two concepts together are promising through the application of $CO_2$ injection for enhanced hydrocarbon recovery and sequestration. The use of

* Corresponding author. Tel.: +61 421000308.
E-mail addresses: c.hussen@postgrad.curtin.edu.au, chawarwan_hussen@yahoo.com.au (C. Khan).

Peer review under responsibility of Egyptian Petroleum Research Institute.

ELSEVIER Production and hosting by Elsevier

1110-0621 © 2013 Production and hosting by Elsevier B.V. on behalf of Egyptian Petroleum Research Institute.
Open access under CC BY-NC-ND license. http://dx.doi.org/10.1016/j.ejpe.2013.06.002

$CO_2$ in enhanced oil recovery had proven to be a technical and economic success for more than 40 years, but the same had not been applied for enhanced gas recovery and storage [18]. Although, the idea for EGR had been around for more than 10 years, meanwhile, it had not been well recognized yet and also it has not been put into practice economically [9,5].

To obtain additional comprehension about these two approaches, current literature reviews had been studied, typically about these two approaches for two similar processes such as storage and enhanced recovery. As a result, there were some features of natural gas reservoirs well understood as oil reservoirs [4]. In terms of geological carbon sequestration, natural gas reservoirs are considered to be more preferable than oil reservoirs (source). For instance, for both natural gas and oil reservoirs two points of view could be demonstrated, natural gas reservoirs were considerably able to store more quantities of $CO_2$ than depleted oil reservoirs with the consideration of both reservoirs with the same volume of hydrocarbon initially in place. First of all, ultimate gas recovery (about 65% of initial gas in place) was almost about two times that of oil (average 35% of initial oil in place). Second, gas was some 30 times more compressible than oil or water [12]. Thus, natural gas reservoirs came into view to be nearly more utilizable for this concept. However, displacement of natural gas by supercritical $CO_2$ had not been properly investigated [20].

## 2. Feasibility of $CO_2$ for enhanced gas recovery

In this section research studies had been reviewed to evaluate the feasibility of displacing natural gas with supercritical $CO_2$. The process of $CO_2$ injection into natural gas reservoirs was still at very early stage of development [16]. Economically, it was highly costly process and highly risky in terms of the outcome and the field contamination [9]. The concern was associated to that the initial gas in place was mixed with the injected $CO_2$ and will be degrading gas production [13]. Technically, the issues caused by mixing of $CO_2$ and natural gas were believed to be one of the reasons why the process of $CO_2$-EGR had received far less attention [4]. Because under the case of gas–gas mixing the injected $CO_2$ made its way to the production wells which is called $CO_2$-breakthrough, at this stage, natural gas production started to drop noticeably and production rate of $CO_2$ began to increase significantly [7].

For those reasons, some barriers should be overcome to stimulate favorability $CO_2$ capture and storage (CCS) adoption under the case of $CO_2$-EGR. Reduction in the costs involved in the entire cycle of CCS, in particular cost of $CO_2$ capture which is the most costly part of the whole $CO_2$ sequestration process [15]. Technology wise, this achievement directly depends on a further study and development in the procedures of $CO_2$. In addition, another concept of $CO_2$ reduction was the implementation of the suggested statement by Kyoto Protocol [19]. If this concept were applied nationwide, carbon credit might partially or fully offset the costs of $CO_2$ storage [8]. These two concepts technology wise and carbon credit wise were the areas that potentially hold the most promise in lowering the overall cost in terms of $CO_2$ injection process as well as reducing $CO_2$ emissions.

Despite of the fact that $CO_2$ and natural gas were mixable, their physical properties were potential favourable for reservoir repressurization without extensive mixing which was beneficial the process of $CO_2$-EGR [16]. For instance, $CO_2$ had density higher than methane by 2–6 times higher at all relevant reservoir conditions. In addition, $CO_2$ had a lower mobility ratio compared to methane, thus it was considered as a high viscosity component [3]. Due to the favorability of these to two $CO_2$ properties, $CO_2$ would be migrated downwards and this relatively would stabilize the displacement process between the injected $CO_2$ and methane initially in place [17]. Another attractive physical property of $CO_2$ was the solubility factor. Carbon dioxide was potentially more soluble than methane in the formation at reservoir conditions. Potentially, it would delay the occurrence of $CO_2$ breakthrough [3]. As a consequence of this, it had been suggested to place or locate the injection wells at the bottom layers of the reservoir. In addition, the production wells are placed at the upper layers of the reservoir to allow a gravity effect for $CO_2$ injection [7]. Surface wise, it was helpful to situate the producer wells as far as possible away from the injectors to delay the occurrence of $CO_2$ breakthrough for as long as possible before mass transfer allowed gas–gas mixing [16,7].

In general, it was a fact that reservoir heterogeneity caused an increase in $CO_2$ breakthrough to the production wells. On the other hand, reservoir re-pressurization could be considered as an additional support against $CO_2$ breakthrough. The benefit of reservoir re-pressurization was that it could happen prior to $CO_2$ breakthrough [18].

Clearly injection from the commencement of hydrocarbon production was risky as the phase behaviour of the reservoir was mostly unknown. By contrast, injection near the end of field life, when the reservoir was becoming depleted, was costly due to high expenses associated with the field rehabilitation [4]. An optimal strategy was to take advantage of high $CO_2$ viscosity and density, reservoir re-pressurization and injecting $CO_2$ into lower portions of the reservoir to produce the maximum levels of methane and minimum levels of $CO_2$ in the upper layers prior to breakthrough [5].

Overall, $CO_2$ characteristics compared to methane delayed $CO_2$-breakthrough and made the process of $CO_2$-EGR more attractive. This phenomenon of gas–gas mixing could be supervised via good reservoir management and production control measures [9], because the physical properties of $CO_2$ undergo changes as the pressure was increased. Therefore, a good estimation of enhanced gas recovery was only preferable to be evaluated by utilizing reservoir simulation software and modelling with the considerations of a substantial and wide range of data. To accomplish this end, numerical simulations of $CO_2$ injection and enhanced gas recovery were investigated using the 'Tempest' reservoir simulator, with input data based on experimental data produced by Clean Gas Technology Australia.

## 3. Reservoir simulation model

The base reservoir model used in this study was based on a known field in the North West Shelf. It was composed of sandstone which had homogeneous layer-cake geology and contained natural gas at a depth of 3650 m. Reservoir core samples were studied experimentally to accurately estimate the general petro-physical characteristics of the reservoir. The physical properties for each one of the tested cores were used as the base assignment to represent the geological model. The reservoir properties were then allocated throughout the reservoir simulation based on the interpretations of each pore plug. The gas reservoir model was created and controlled by variousness of cell distributions in terms of width, length and thickness.

The dimensions of the geological model, in the *X*-grid 17 grid-blocks were used and 22 grid-blocks were used in the *Y* direction. The divisions in the *Z* directions vary by layers, with 4, 3, 6 and 5 grid-blocks were formed to represent layers L1, L2, L3 and L4, respectively. The parameter values are distributed in such a way, for closeness to reality.

Starting from the upper part of the geological model, thickness of the first layer was 50 m, and it had a value of 0.04 porosity, 0.05 for critical gas saturation and 0.120 for critical water saturation. The permeability values distributed as 6, 6 and 4 md for *x*, *y* and *z* directions, respectively. For the second layer from the top of the reservoir, it had a thickness of 70 m. Porosity, critical gas and water saturations values for the existence thickness were determined as 0.17, 0.03 and 0.175, respectively. In addition, permeability values for this layer were distributed as 390, 390 and 370 md for *x*, *y* and *z*. The third layer of the reservoir model was organized as porosity of 0.14, gas critical saturation with a value of 0.04 and 0.145 for critical water saturation with a thickness of 120 m. The bottom layer was also characterized by a porosity of 0.09, a critical gas saturation of 0.04 and a water saturation of 0.100. Permeability for the three directions of the last layer was presented as 8.5, 8.5 and 6 md for *x*, *y* and *z* respectively Thus, the arrangement of the layers from top to bottom of the reservoir model starts as very low, high, medium and low quality rock, respectively. Each of the geological layers was represented by different grid layers in the model, as shown in Table 1.

In terms of gas/water contact, reference depth of the reservoir, pressure and temperature at the reference depth and depth specifying the water–gas contact were calibrated to achieve the equilibrium initialization. This provided indications of a transition zone between gas and water. As a result the simulator would take these values into account and stabilize the initial aquifer zone, which was allocated in depths of the bottom cells in the gas reservoir model. Beneath of this aquifer zones was the target for drilling and completion at the injector wells.

In general, the modelled aquifer in the subsurface of this gas reservoir met the physical conditions of aquifers. First of all, the top layer of the aquifer was at a depth of "4400 m". Source [8] claimed that aquifer beyond the depth of 800 m made $CO_2$ to act as a supercritical fluid and it would have density as high as that for water. In addition, $CO_2$ density in aquifers with a depth of greater than 3500 was higher compared to that of sweat water. In addition to the aquifer, the location and depth completion of the injection wells might have sufficient permeability and porosity to resist keeping the injected $CO_2$ in the aquifer.

$CO_2$ injection at the gas–water contact of the reservoir model had a potential to act as a substitute support for pressure maintenance, thereby allowing simultaneously the production of gas. In addition, it was anticipated that the process would improve displacement efficiency and resulting in an increased ultimate recovery factor [11]. In order to understand the impact of the reservoir geology on potential development schemes, the initial composition, the development of rock layers and properties were modelled using the "tempest" reservoir simulation software.

The simulation process used the 'Solvent' option of the reservoir simulator, an extended black-oil model in which the components coexisted. The simulation standard compositions (SCMP) were reservoir gas (RESV) and solvent gas (SOLV). The reservoir gas depicted the mole fraction of the components in the mixture of the gas reservoir, which originally represented the initial gas in place. The solvent gas specified the solvent concentration in the injected gas ($CO_2$). The initial pressure of the reservoir model is set at 406 bar, and temperature of 160 °C. 'PVT-Software' was used to generate the necessary PVT data for simulation. Table 1 shows the different porosity, absolute permeability, critical gas saturation (Sgcr) and critical water saturation (Swcr) for each layer. Furthermore, the relative permeability curves are generated using Darcy's Law to achieve the displacement between the gases.

The development of the geological model was designed to illustrate optimization of the initial gas recovery in place. In order to determine the optimal development plan and to test its robustness over the uncertainty range of reserves, a number of dynamic reserve simulation models were constructed. Over all, for all scenarios the initial component names in the gas mixture were listed as $C_1$, $C_2$, $C_3$ and $CO_2$. A mole fraction or initial composition of each one of the mentioned components was 0.9, 0.005, 0.005 and 0.09, respectively as shown in

**Table 2** Reservoir model parameters.

| Property | Value |
|---|---|
| Reservoir type | Sandstone |
| Reservoir depth | 3650 m |
| Area (*X*–*Y* direction) | 1700 m *x*, 2300 m *y* |
| Thickness (*z* direction) | 300 m |
| Grids in *X* direction | 17 |
| Grids in *Y* direction | 22 |
| Grids in *Z* direction | 4, 3, 6 and 5 for L1, L2, L3 and L4 |
| Relative permeability | JBN method and Darcy's law |
| Initial reservoir temperature | 160 °C |
| Initial reservoir pressure | 406 bar |
| Well injector pressure (maximum) | 450 bar |
| Well producer pressure (minimum) | 50 bar |
| $CO_2$ injection rate | 2422.5 and 1275 $1000 \times m^3$/day |
| $C_1$ production rate | $25{,}500 \times 1000\ m^3$/d |

**Table 1** General reservoir characteristic by layer.

| Layer | *Z* thickness (m) | *Z* direction (cells) | Kx (md) | Ky (md) | Kz (md) | Porosity (%) | Sgcr | Swcr | Core plugs |
|---|---|---|---|---|---|---|---|---|---|
| L1 | 50 | 4 | 6 | 6 | 4 | 0.04 | 0.05 | 0.120 | S_A_4 |
| L2 | 70 | 3 | 390 | 390 | 370 | 0.17 | 0.03 | 0.175 | S_A_1 |
| L4 | 120 | 6 | 115 | 115 | 100 | 0.14 | 0.04 | 0.145 | S_A_2 |
| L4 | 60 | 5 | 8.5 | 8.5 | 6 | 0.09 | 0.05 | 0.100 | S_A_3 |

**Table 3** Compositional table.

| Component | Composition |
|---|---|
| $CO_2$ | 0.09 |
| $C_1$ | 0.9 |
| $C_2$ | 0.005 |
| $C_3$ | 0.005 |

Table 3. Production of these gases could be economically advantageous and replacing the produced gas would allocate extra space for further $CO_2$ deposition.

In addition, a simplified gas layered model in which the components coexist consists of $1.7 \times 2.2 \times 0.3$ km grid cells (see Table 2). The rock properties, well properties and completion were assigned to the various thicknesses in the layers across the grids in order to properly model the fluid flow in the neighbourhood of the production wells.

The base case development plan calls for three vertical production wells and allocated in the upper layers of the reservoir and their perforation locations were differently placed with various vertical lengths according to the structure of the layer. These production wells were expected to produce natural gas at different rates. In general, the production wells were controlled as a function of a maximum gas production rate per day and a minimum producing bottom-hole pressure for each well. The summation of the production rates for each one of the wells was equivalent to the total gas production per day "$25{,}000 \times 1000\ m^3/d$" of the reservoir simulation.

The simulation suggested that there is sufficient vertical permeability in the reservoir to allow the gas in the lower portions to move towards the wells. Two gas injector wells were proposed to dispose of the produced $CO_2$ by re-injecting it into the gas reservoir down-dip of the production wells. The perforated locations of the wells would be at a distance such that $CO_2$ breakthrough at the production wells was after the plateau production [21]. By contrast to the producer wells, the two injection wells were perforated in the bottom layer beneath the zone of G/W contact in order to take the gravity effects into account. This potential had enough capacity to handle breakthrough volumes as wells as $CO_2$ re-injection as shown in Table 4.

### *3.1. Three-dimensional simulation of a base-case*

The simulation grid, reservoir physical properties and initial equilibration statue incorporated and the layout is displayed in Fig. 1. The objective is to investigate the influence on the flow through the main reservoir characteristic units, like porosity, permeability, water and gas saturation, $CO_2$ injection rates and also $CO_2$ production rate in the gas production. In addition to this case, the maximum gas production was set at 7500, 8500 and $9000 \times 1000\ m^3$/day for wells number 1, 2 and 3, respectively. In order to test the model, the reservoir layers estimated to be filled with a homogeneous gas mixture (Table. 3). Simulation of natural gas production without any injection was performed for a base-case under normal production conditions in such a way that the bottom-hole wells pressure decline at a time period of 20 years. Therefore, a number of 3D geological models were constructed to reflect potential variations in the reservoir distribution such as reference pore volume; water and gas phase saturation (Fig. 1).

In this way the full range of the reservoir was carried through the dynamic reservoir modelling. As a consequence, the proposed development scenarios could be optimized over the range of the reservoir uncertainty and also illustrate the

**Table 4** Well placement and completion depth.

| Well | Type | $X$ (m) | $Y$ (m) | MD (m) | Completion (m) | RAD (m) | Layer |
|---|---|---|---|---|---|---|---|
| I-1 | Injector | 650 | 150 | 4394–4683 | 4639–4683 | 0.5 | L4 |
| I-2 | Injector | 1650 | 2250 | 4554–4843 | 4799–4843 | 0.5 | L4 |
| P-1 | Producer | 1350 | 650 | 3716–4004 | 3768–3822 | 0.5 | L2 |
| P-2 | Producer | 1050 | 1250 | 3648–3924 | 3701–3754 | 0.5 | L2 |
| P-3 | Producer | 450 | 1650 | 3676–3964 | 3728–3782 | 0.5 | L2 |

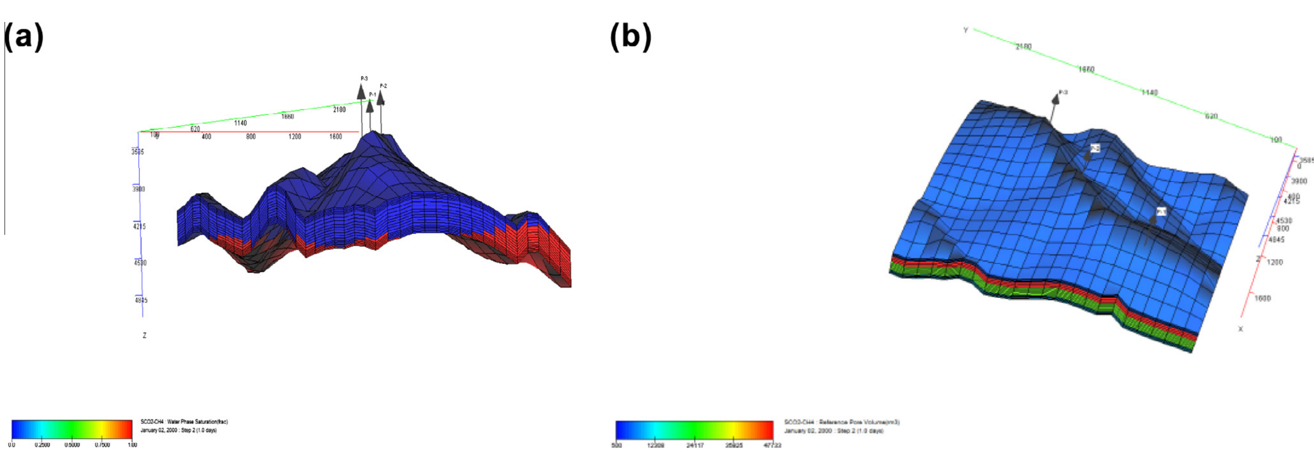


**Figure 1** construction of geological model. a1: water and gas phase saturation b1: reference pore volume.

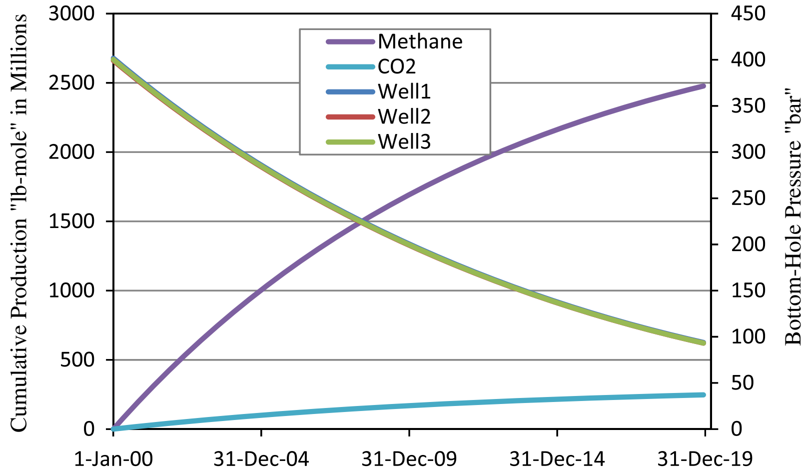


**Figure 2** Bottom-hole pressure and cumulative gas production versus time.

sweep efficiency of $CO_2$ injection. Additionally, cumulative methane and $CO_2$ production "lb-mole" and bottom-hole pressure "bar" was estimated for this case over the estimated 20 years (Fig. 2). This case was intended to be the basis for comparison, to illustrate the acceleration of methane production, and lower $CO_2$ production under a case of $CO_2$ injection as a function of given various rates and times of injection. The bottom-hole pressure BHP was measured in this case and under a late stage of $CO_2$ injection, the measured BHP decline was used to determine the time start of $CO_2$ injection as shown in Fig. 2.

### *3.2. Optimization of gas recovery and $CO_2$ storage*

The subsurface development plan had been designed to optimize the recovery gas in place and storage. The injection wells 1 and 2 with vertical depths were 4394–4683 and 4554–4843 m, respectively and would be used to minimize drawdown and ensure good sweep. The production wells 1, 2 and 3 are also with vertical sections at depths of 3716–4004, 3648–3924 and 3676–3964 m, respectively in terms of the hypothetical reservoir model (Fig. 3).

The produced $CO_2$ would be disposed by means of a re-injection well down dip of the injectors. The principal aim of the simulation is to illustrate a re-injection strategy of an optimal $CO_2$ injection for enhanced gas recovery and $CO_2$ storage. This purpose was investigated through determining the optimum injection target rate, the time response of $CO_2$ injection and as a result, illustration of mixing rates between the gases.

The simulation model had been used to test whether the chosen development plan was optimal of the range of reserve expected and robust under different assumptions for key parameters in the reservoir description. Re-injection of the produced $CO_2$ into a down-dip location of the gas reservoir model had been established as the preferred disposal method. The injected $CO_2$ was expected to migrate to the bottom layers due to its high density. The location for the $CO_2$ injectors potentially was chosen to ensure both containment of injected gas with the identified structure and a suitable delay time prior to breakthrough at the production well location. Uncertainties in this re-injection strategy were the timing of $CO_2$ breakthrough at the producing wells. Since the natural gas and the re-injected $CO_2$ would not re-mix together with the initial

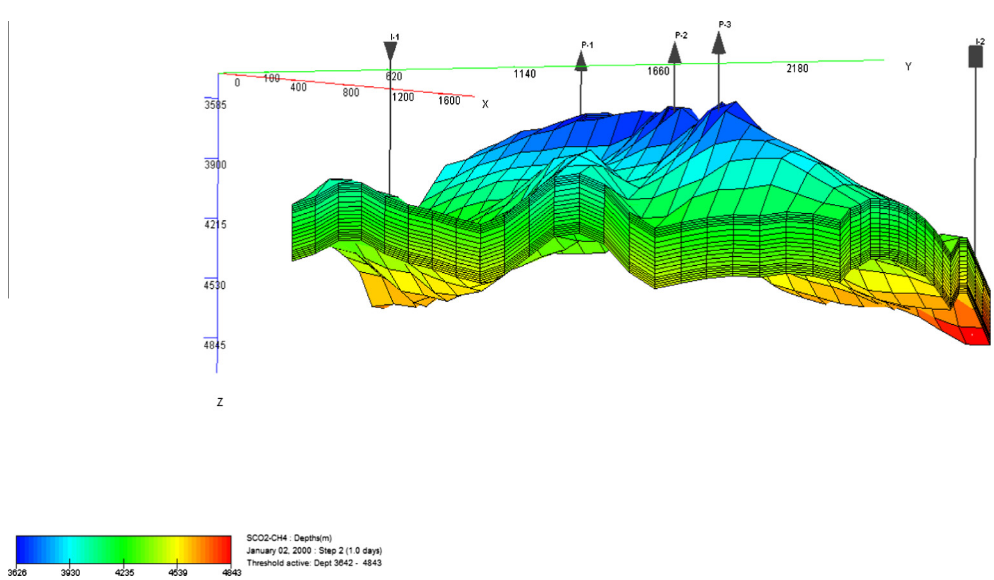

**Figure 3** Hypothetical gas reservoir model.

natural gas in place could over-run the re-injected $CO_2$ to reach the production wells [21].

Accordingly, $CO_2$ breakthrough at the producer wells was not expected to occur until after the end of the plateau production period, in this manner avoiding any impact on natural gas production. In addition, production was expected to be influenced strongly by the aquifer zone and vertical completion of the injector well in the lower layers of the zone potentially had impact on breakthrough and as a result sufficient recoveries are expected.

The total reference pore volume had been estimated at 1,439,786,000 $rm^3$ by using a conditional simulation tool. The recovery factor was based on selection of gas production from the wells. Based on variations in the structural and stratigraphic model range estimations of the recovery factor was different from one well to another. The recovery efficiency ranges were put together in order to establish the ultimate recovery over the life of the field as reservoir producing. To achieve this task, different case scenarios were run for 20 years in order to investigate the case study where a miscible $CO_2$ injection was considered for enhanced gas production and storage from the gas reservoir model.

### *3.3. Case scenario one*

In this case, $CO_2$ injection was modelled and potentially allowed significant impacts on fluid density such as temperature and pressure gradient in the injection system as a function of depth variation of reservoir and gravity effects.

Under the base-case, the initial gas production from this gas reservoir model was started in January 2000 through Wells 1, 2 and 3. The pressure declined gradually from its initial pressure of 401 bar as a response to the gas production. Accordingly, two injector wells were used as disposal wells to re-inject the initial $CO_2$ production directly into the formation instead of being emitted into the atmosphere. Thus, $CO_2$ was re-injected in a liquid-like state into the gas reservoir at a rate of 1125 and $1125 \times 1000$ $m^3$/day for each injector.

The maximum gas production rates for each one of the producer wells was set as it was under the base-case. This case was tested through the reservoir simulation at different maximum injection rates for the simulation, as it is shown in Table 5.

**Table 5** Production and injection rates of the case scenarios $1000 \times m^3/day$.

| Case scenario one at high injection rate | | | |
|---|---|---|---|
| Well-1 | 7500 | Well-1 | 1125 |
| Well-2 | 8500 | Well-2 | 1125 |
| Well-3 | 9000 | – | – |
| Total production rate | 25000 | Total injection rate | 2550 |
| *Case scenario one at low injection rate* | | | |
| Well-1 | 7500 | Well-1 | 637.5 |
| Well-2 | 8500 | Well-2 | 637.5 |
| Well-3 | 9000 | – | – |
| Total production rate | 25000 | Total injection rate | 1275 |
| *Case scenario two at high injection after conversion* | | | |
| Well-1 | 12250 | Well-1 | 750 |
| Well-2 | 1275 | Well-2 | 750 |
| – | – | Well-3 | 750 |
| Total production rate | 25000 | Total injection rate | 2550 |

This potential allowed simultaneously enhancing the initial gas production and maintaining initial reservoir pressure during production. For this case the simulations were run with and without considering solubility factor as shown in Fig. 4.

The results of the simulation suggest that without $CO_2$ dissolution in the formation water, Fig. 4 shows the $CO_2$ breakthrough points to be in 30 December 2001 (Production Well 1), 29 September 2002 (Production Well 2), 27 September 2003 (Production Well 3). In comparisons to these dates with the case of solubility, the simulation indicates breakthrough on 30 March 2002, 29 December 20025 and 28 March 2004 for production wells 1, 2 and 3, respectively. This comparison demonstrated the maximum methane production and the fraction of $CO_2$ remaining in the reservoir.

The comparisons between the scenarios indicated that the solubility of $CO_2$ was greater than methane at all relevant pressures and temperatures. This implied a reduction in the volume of $CO_2$ available in the gas reservoir to mix with methane, which potentially delayed $CO_2$ breakthrough. The effect of $CO_2$ solubility obtained in this study accords with [3]. Thus, in the following cases only the scenario of solubility is taken into account.

The simulation results showed that after the $CO_2$ started to breakthrough, the $CO_2$ production started to increase dramatically to reach 536,373,000 lb-mole as compared to the initial $CO_2$ production of 526,961,000 lb-mole with no $CO_2$ injection. But before reaching to this stage, in the beginning of gas production the total $CO_2$ production rate was lower than the total $CO_2$ injection rates. Thus, further $CO_2$ lb-mole/day was required from a power plant nearby in order to reach the desired volume rate of $CO_2$ injection. The additional required amount of $CO_2$ from the sources was declined with time after the $CO_2$ breakthrough. Secondly, $CO_2$ injection was simulated at a lower rate of $637.5 \times 1000$ $m^3$/day for each injector while the gas production rates for each producer were the same as for the high injection scenario.

As a result of the simulation, time of $CO_2$ breakthrough was estimated. From this timing, the best injection rate of $CO_2$ in terms of methane and $CO_2$ production was determined over the estimated period of time. The average bottom-hole pressure ‘‘bar’’ and total cumulative gas production rate ‘‘lb-mole’’ of the three production wells are illustrated for the two different injection rates (in Fig. 5).

In terms of the enhanced gas recovery and the reservoir re-pressurization, a comparison between the two different injection rates indicated the gas recovery factor in the first scenario is greater than that in case scenario 2 and the base-case. This illustrated that, the higher was the rate of $CO_2$ injection the greater recovery efficiency is achieved. On the other hand, Fig. 6 demonstrated different times of $CO_2$ breakthrough under different injection rates and indicate that the high injection rate of $CO_2$ the earlier breakthrough occurred.

As a result the, the simulation suggested that even though $CO_2$ injection excessive gas mixing, at the same time it has potential to increase the incremental gas recovery. It is worth mentioning that the initial gas reservoir pressure was high and even though, the production wells were allocated at the same layer, but their depth completions were different from each other. Therefore, we anticipated some compositional gradient due to gravity and temperature effects generated by the depth variation and high density contrast of $CO_2$ as compared to methane. Some evidence of compositional variation was

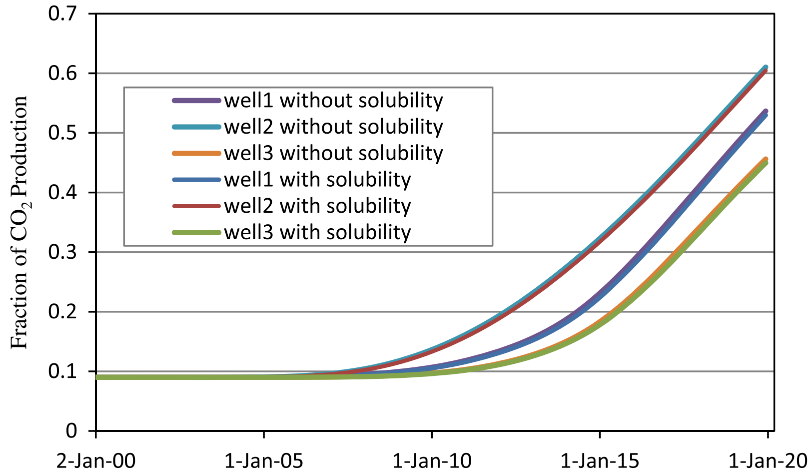


**Figure 4** A comparison of $CO_2$ breakthrough with and without solubility consideration.

observed between the producing wells in terms of $CO_2$ content, however this variation was very minimal as compared to the fraction initially in place in the reservoir. Thus the produced fraction of $CO_2$ in each well was seen as a straight line from the beginning of production (see Fig. 6).

### *3.4. Case scenario two*

This case scenario attempts to find $CO_2$ injection timing for comparison with the recovery factors in the above scenario using the data obtained experimentally. In this case, reservoir heterogeneity accelerated the $CO_2$ breakthrough in the production well, and of course reservoir re-pressurization was considered as additional support for mitigation against $CO_2$ breakthrough. Accordingly, $CO_2$ was re-injected at the high rate $2250 \times 1000\ m^3$/day based on the normal case, when the bottom hole pressure of the production wells decline to about 280 bar in March 27, 2005 (see Fig. 2).

That is, only a fraction of the methane was produced before injection. However, after almost five years of gas production, $CO_2$ was re-injected back into the reservoir at the high rate to re-pressurize and increase incremental gas recovery, resulting in continuation of gas production for the wells. The first production well that shows $CO_2$ breakthrough is automatically shut-in at that time. When the concentration of $CO_2$ in the produced gas reached 20% in June 14, 2014, the shut-in production well (Well 2) was converted to become Injector 3, this was to accelerate methane production, with less $CO_2$ production for the life of the reservoir. The converted well will have a changed depth completion from the second layer to the bottom layer of the reservoir.

In terms of the reservoir model under the second case scenario, the maximum gas production rate was set at $25000 \times 1000\ m^3$/day. In the beginning of gas production there were three gas producer wells. The maximum gas production rate of each producer well set at $(7500, 8500$ and $9000) \times 1000\ m^3$/day for the gas producer wells 1, 2 and 3, respectively. At the announcement stage of injection, the maximum injection rate of $CO_2$ for the injector wells was $2250 \times 1000\ m^3$/d as it was under the first case scenario.

After the conversion of the producer well, the gas production rate of the producer wells was re-set at $(11750, 0$ and $13250) \times 1000\ m^3$/day for the well 1, 2 and 3, respectively and the injection rate was re-set at a rate of $750 \times 1000\ m^3$/day for each one of the new and the old injector wells (Table. 5). In the year of 10 Jun 2017, the producer well 1 was also stopped from production. After the cessation of producer 1, natural gas will be produced only from well number 3 at a rate

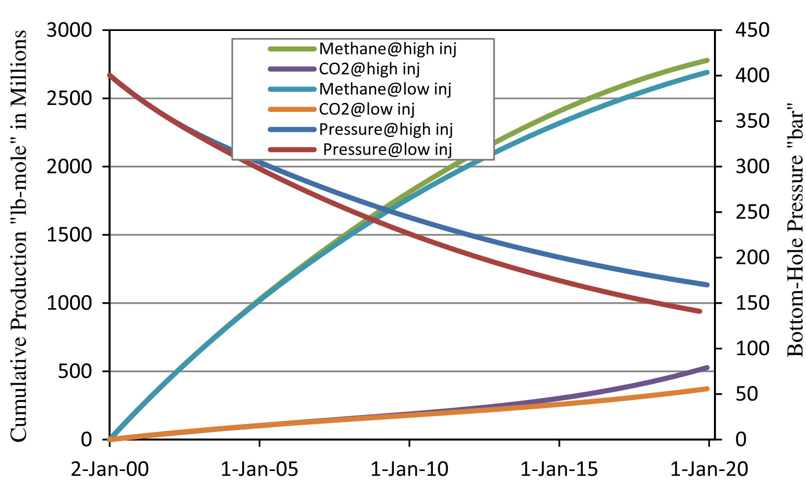


**Figure 5** Bottom-hole pressure and cumulative gas production versus time at high and low $CO_2$ injection rate.

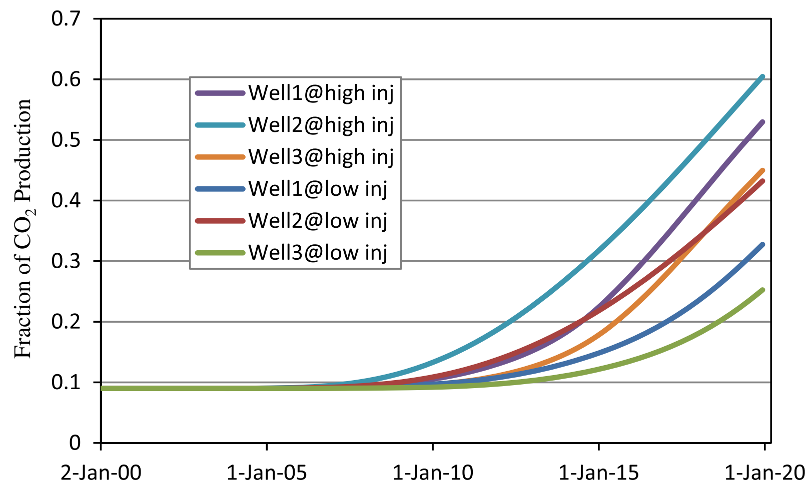


**Figure 6** $CO_2$ breakthrough at different injection rates.

of $25000 \times 1000$ m$^3$/day. Furthermore, the last production well and the other injectors were ceased on 11 March 2018.

Fig. 7 shows the remaining production wells (1 and 3) which will be shut-in during the years 2017 and 2018, respectively when the $CO_2$ production rate for each well reaches 30%, so as to reduce $CO_2$ production as much as possible and achieve economic feasibility.

The total cumulative methane and $CO_2$ production for the wells is illustrated in Fig. 8 in terms of 30% of $CO_2$ production. The timing of the events had an important role in illustrating the optimum injection rate strategy. Higher and later injection rates appeared to be near the optimum strategy. First, the higher recovery factor was achieved in less time compared to the base-case. Second, with late injection less $CO_2$ w required compared to the second scenario, resulting in reduced costs. Finally, the effects of the different scenarios on $CO_2$ storage were demonstrated in the following sections.

### 4. Dissolution of $CO_2$ in formation and storage

Storage volumes of $CO_2$ were documented by using a well established mass balance method developed through the results of the reservoir simulation. This method qualifies the volume of $CO_2$ initially in place and tracks the changes in the producible volumes as reservoir management techniques, when $CO_2$ injection is applied during the life of the field. Estimation of $CO_2$ storage was based on the idea of $CO_2$ breakthrough for the production wells. It was assumed that 9% of $CO_2$ was present in the reservoir and 90% for methane. Fig. 9, depicts the produced $CO_2$ fraction in the reservoir during the process of production for producer well 1 under the base-case when there was no injection with and without considering solubility. As it can be seen, the produced fraction of $CO_2$ was declining when solubility is taken into account.

In addition, Fig. 9 also depicts the total produced $CO_2$ fraction in the reservoir when there were different injections of $CO_2$ at different stages only with consideration of $CO_2$ solubility. As a result, when there was injection, the produced fraction of $CO_2$ is increased due to the produced fraction of injected $CO_2$.

Under the case of late injection, the total $CO_2$ fraction of the wells fluctuated at the end of the years due to cessation of wells 1, 2 and 3 when $CO_2$ concentration exceeded 30% and 20% in 14-Jun-2014, 10-Jun- 2017 and 11-Mar-2018.

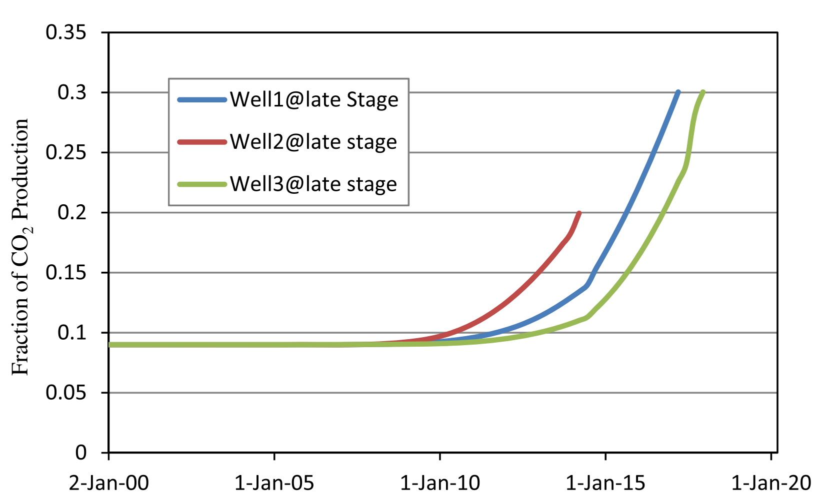


**Figure 7** $CO_2$ breakthrough of high injection at late stage of $CO_2$ injection.

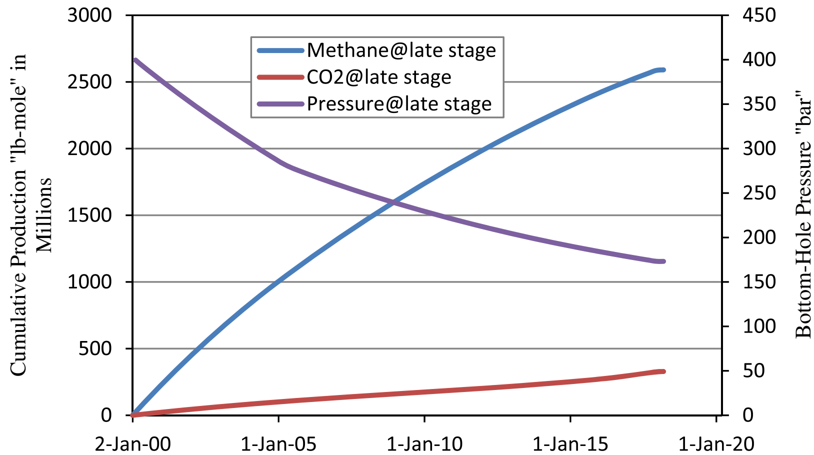


**Figure 8** Bottom-hole pressure and cumulative gas production versus time at late stage of $CO_2$ injection.

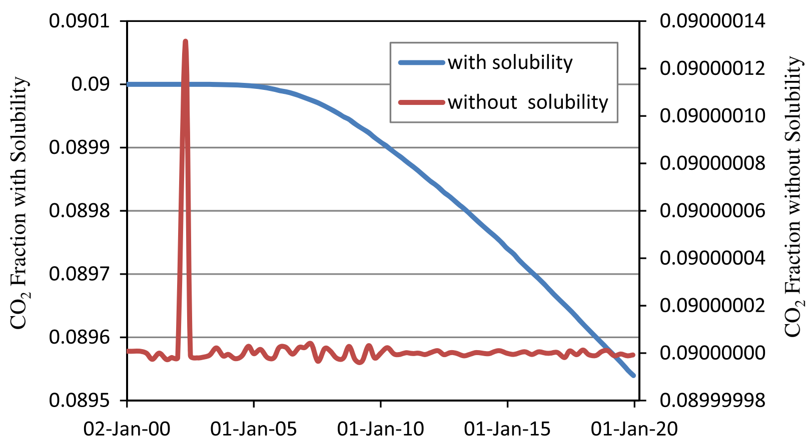


**Figure 9** Fraction of $CO_2$ production under the base-case.

When the concept of $CO_2$ breakthrough was illustrated, during $CO_2$ re-injection process the fraction of the produced $CO_2$ that exceeds the $CO_2$ fraction initially had been presented in the reservoir will represent the produced fraction of the injected $CO_2$ ($PFICO_2$) (Fig. 10).

In addition, the higher $CO_2$ injection, the more fraction of the injected $CO_2$ was produced. Thus, the more produced fraction of the injected $CO_2$ the lower volume of the injected $CO_2$ was stored. Fig. 11 shows different injection rates at different stages of injection for all the cases and also illustrates gradual increases in $CO_2$ injection rates, until each case reaches the required rate of $CO_2$ injection. Under the stage of late injection, the injected $CO_2$ reaches to the required rate of $CO_2$ injection faster than the other cases. This was due to the gas production before the commencement of $CO_2$ injection. Therefore, when $CO_2$ injection started, the injected $CO_2$ displaced the natural gas already produced from the gas reservoir and after a few months reached the desirable rate of injection.

$CO_2$ storage was evaluated after when the concept of $CO_2$ breakthrough was illustrated for the two case scenarios in terms of the produced fraction of injected $CO_2$ $PFICO_2$ and $CO_2$ component originally present in the gas reservoir. After the estimation of the $PFICO_2$ for each one of the cases, the production rate of the injected $CO_2$ was calculated by multiplying the $PFICO_2$ by the production rate of $CO_2$ during $CO_2$ injection. In addition, a difference between the production of the injected $CO_2$ and the injection rate evaluated $CO_2$ storage of the injected $CO_2$ for each one of the cases (Fig. 11). As it can be seen, the higher injection rate the higher volume of $CO_2$ storage was achieved.

During the $CO_2$ injection process, a part of the injected $CO_2$ dissolves in the formation water. Therefore, an important consideration was solubility of $CO_2$, which was strongly associated with the pressure. Accordingly, to illustrate this concept, as an optimum case consideration, the first case scenario with the highest injection rate was demonstrated with and without considering the solubility factor.

To demonstrate the concept of $CO_2$ dissolution in the formation water presented in the reservoir mode, a comparison of $CO_2$ production with solubility factor was taken into account as well where solubility is not considered (Fig. 12). This comparison was depicted in terms of re-production rate of the $CO_2$ injection and $CO_2$ storage (Figs. 13 and 14).

Over all, Fig. 12 demonstrated $CO_2$ production rates "lb-mole/day" and differences between the two cases. However, there was a slight difference between these two scenarios which was almost indiscernible in a visual inspection of the plotted lines. Therefore, the difference curve in production rate was

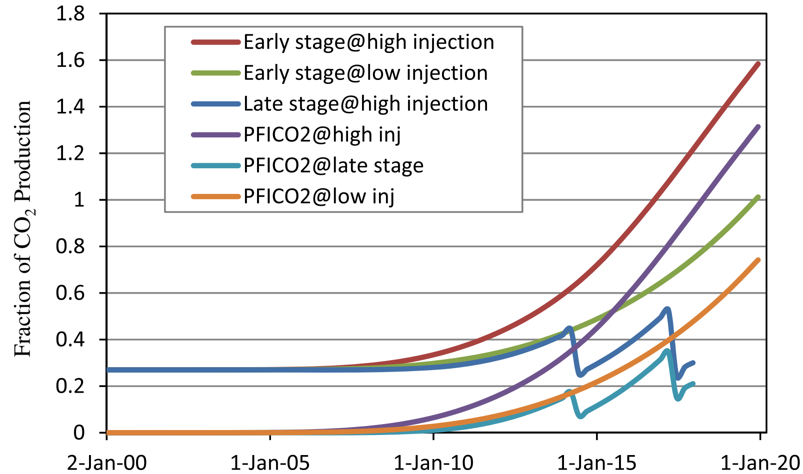


**Figure 10** Total fraction of $CO_2$ production and fraction of the injected $CO_2$ under different case scenarios.

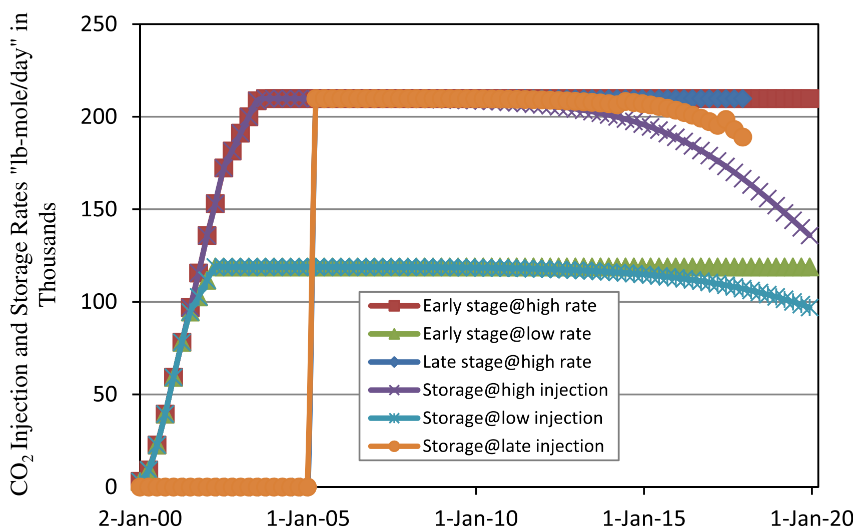


**Figure 11** $CO_2$ injection rate and storage under different case scenarios.

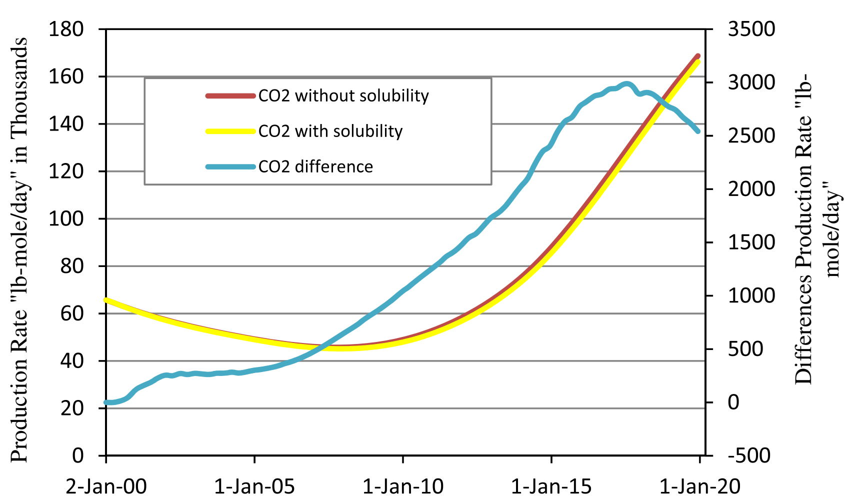


**Figure 12** $CO_2$ production rate "lb-mole/day" at high injection rate based on solubility considered and not considered.

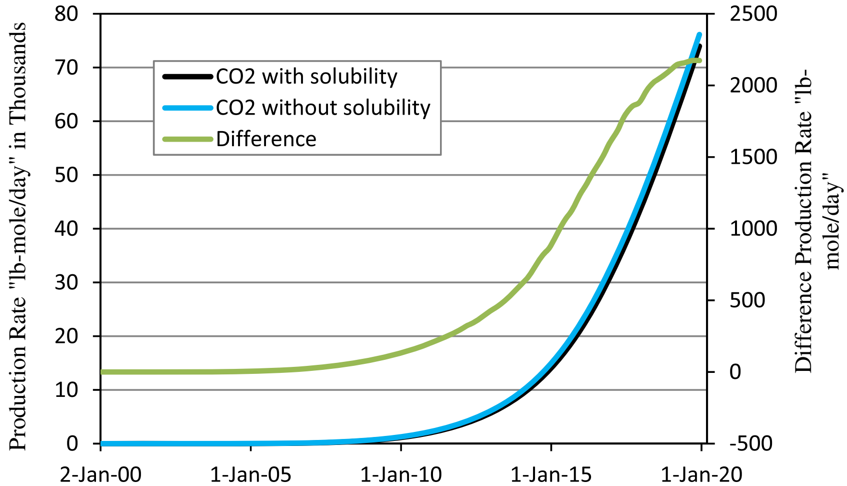


**Figure 13** Production rate of the injected $CO_2$ "lb-mole/day" at high injection rate based on solubility considered and not considered.

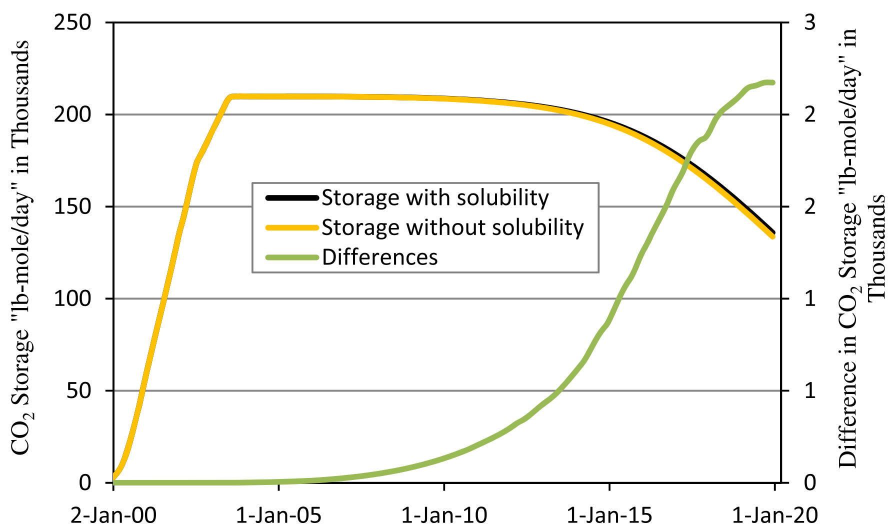


**Figure 14** $CO_2$ storage at high injection rate based on solubility considered and not considered.

also plotted to highlight the difference in $CO_2$ production due to solubility.

Generally, the production rate will decline with a reduction in reservoir pressure. As shown in Fig. 12, the $CO_2$ production rate was higher without solubility (red curve) compared with the solubility case (yellow curve) over the same estimated period of time. The blue curve represented the level of $CO_2$ reduction when solubility was considered, in other words it represented the production differential between the two above cases. The $CO_2$ content in the production (yellow curve) started to increase at a slower rate than the non-solubility case (red curve). The differential started to decline due to saturation of the formation of water with the injected $CO_2$.

Fig. 13 illustrates the production rate of the injected $CO_2$ and the differences for the solubility and non-solubility cases. In case there was solubility, during the process of $CO_2$ injection into the reservoir a smaller amount of the injected $CO_2$ was produced compared to the non-solubility case. For this case, the ratio of $CO_2$ to initial methane in place was continuously increasing due to the re-injection of produced $CO_2$ and the initial $CO_2$ still unrecoverable in the reservoir.

In particular, with solubility more injected $CO_2$ was stored in the reservoir (Fig. 14). That is, the process of $CO_2$ storage remains attractive unless the production rate of the injected $CO_2$ remained below the $CO_2$ injection rate. The higher the $CO_2$ injection rate the greater volume of $CO_2$ available in the reservoir to be dissolved due to high potential for $CO_2$ solubility compared to that of methane. In addition, reasonable $CO_2$ storage was achieved up to the point where the production rates of the injected $CO_2$ was still not equal to the injection rate. Thus, as the stored volume of $CO_2$ declined the more the production rate of the injected $CO_2$ increases (Fig. 14).

## 5. Introduction of carbon credits

In order to make the process of $CO_2$-EGR and storage economically more attractive the costs involved in the process need to be lowered or carbon credit be taken into account. Currently, the cost estimations of $CO_2$ capture and the storage technology CCS is very high. This technology is unlikely to be put into practice effectively without any financial motivation or Tax incentives. Economically it becomes more feasible if it is combined with the process of $CO_2$ capture and storage, this is due to re-injection of the native $CO_2$ production into the reservoir and may result in less $CO_2$ requirement from other source or producers [10].

Overall, the concept of $CO_2$ storage from the same source potential provided a reasonable structure for carbon credit to be fully developed during the process of $CO_2$-EGR and storage. In particular, $CO_2$ capture, separation systems and storage (compression, transportation and injection) systems were considered as an emission reduction approach [14]. A credit for this reduction is reduced by producing additional $CO_2$ per ton injected; possibly released into the atmosphere during the $CO_2$ storage process.

This process $CO_2$ for enhanced gas recovery and sequestration (CEGRS) is likely to take place in the context of carbon credit schemes and development of low value emissions. However, the idea of carbon credit had been around, but world widely had not been put into practice yet despite extensive coverage and political positioning. Therefore, there was no standard method presented in the published studies for calculating carbon credit [8]. So here, the concept was expressed as a function of carbon credit and carbon tax. According to the equation below, the first part of the equation shows the storage of the injected $CO_2$ and multiplied by the carbon credit. This will estimate the received price for per ton of $CO_2$ storage. Accordingly, this part would be estimated in terms of the injection rate of $CO_2$, production rate of $CO_2$ and also production rate of the injected $CO_2$. As a result, this will be considered as the additional source of revenue for the process. The second part of the equation shows the released amount of $CO_2$ into the atmosphere. This section will be evaluated in terms of energy penalty during the process of $CO_2$ storage as a function of the injected $CO_2$. Once carbon tax is considered, this will represent a reduction in the additional source of revenue.

$$Cp = \sum_{n=1}^{N} \left[ \frac{\left[ Mass - \frac{(PFCO_2 - CO_2 IIP)}{PRCO_2^{-1}} \right]}{(CC)^{-1}} \right]_n - \left[ \frac{(EP \times Mass)}{(Ct)^{-1}} \right]_n$$

$Cp$: net carbon credit \$/tonne.$N$: the number of the project years.$n$: is the number of years.CC: carbon credit \$/tonne.PF-$CO_2$: produced faction of $CO_2$ "fraction".$CO_2$ IIP: initial $CO_2$ in place "fraction".$PRCO_2$: production of CO2 tonne/year.EP: energy penalty %.Mass: mass flow rate of $CO_2$ injectionCt: carbon tax \$/tonne

Fig. 11 shows $CO_2$ injection rate and storage per tonne of $CO_2$ under different case scenarios. Based on current literature studies, large variations in unit of $CO_2$ energy penalty or the energy burnt and released into the atmosphere were mentioned and ranged from 13.0% to 25.0% according to the implemented technology for $CO_2$ separation and types of the power plan [6]. As a result, with the consideration of the energy penalty % through Fig. 11 emission per ton of $CO_2$ injection can be considered during the process of $CO_2$ capture and sequestration.

Where the result of the carbon credit markets come into existence in any significant way as a reduction of one ton of $CO_2$ fossil emissions by either preventing it from the atmosphere (natural gas reservoir) or by extracting it out of the atmosphere (power plan). The storage site will represent additional source of revenue and the amount of $CO_2$ emission represents additional cost. We estimated that the difference between them represented net carbon credit.

If future $CO_2$ markets involved effective payment for $CO_2$ storage compared to carbon tax for $CO_2$ emission, the introduction of a carbon credit scheme can be considered as additional source of revenue or the re-injection cost recovery. Optimistically, the economic feasibility for $CO_2$-EGR and storage became more attractive [18].

## 6. Results and discussions

The base-case scenario was simulated to enable gas production continuously under normal production conditions. Vertical production and injection wells allocated with different depths with the consideration of aquifer zone beneath the gas reservoir. For the other two case scenarios, $CO_2$ injection into the lower portion of the reservoir technically re-pressurized the reservoir and efficiently swept the natural gas from the bottom layers in the direction towards the production wells, while minimizing contamination and gas mixing in the upper parts of the reservoir.

It is obvious that the higher $CO_2$ injection rate in the layers with high permeability, the higher portions of the injected $CO_2$ took place in the layers. In this case, the $CO_2$ breakthrough occurred faster at the production wells. The breakthrough time was defined as the time when the injected $CO_2$ arrived to the production wells. The volume of $CO_2$ breakthrough was determined as the volume that exceeded the initial volume of $CO_2$ that is supposed to be produced from the reservoir. Lower grids in the bottom layers of the reservoir showed that the faster increase in $CO_2$ concentration was due to gravity, temperature and pressure effects generated by high density of $CO_2$ and depth variations. Technically the simulation results indicated that, the higher injection rate of $CO_2$ can potentially enhance more incremental increases in gas production; however, it will lower the natural gas quality by excessive mixing and early breakthrough creating more $CO_2$ production.

Geologically, injection of $CO_2$ into the aquifer with the depth of 3650 m had strong effects on methane production and $CO_2$ storage due to $CO_2$ density. At this depth, it acted as a supercritical fluid and would have a density as high as water. As expected, the less volume of the injected $CO_2$ was stored when the initial brine of the reservoir was saturated. According to the simulation results, $CO_2$ injection at a higher injection pressure than the initial reservoir pressure increases stored volumes of the injected $CO_2$ considerably, while less methane was produced at the production wells. As a result, feasibility of $CO_2$ injection is a function of aquifer depth, low permeability and brine saturation.

Fig. 15 shows the efficient tendency of $CO_2$ flows downwards and stabilizes the displacement of the native gas due to its physical properties as a function pressure gradient, gravitational effects.

Clearly it can be observed that after some period of injection, the grids around the production wells were covered with the initial natural gas and the reservoir "lower portion" was partially filled with the injected $CO_2$. The heterogeneity of reservoir preferentially flows $CO_2$ from the bottom layer towards the production wells as a function of permeability existence for each layers, especially in the second layer from the top of the reservoir (high permeable). This preferential flow could be

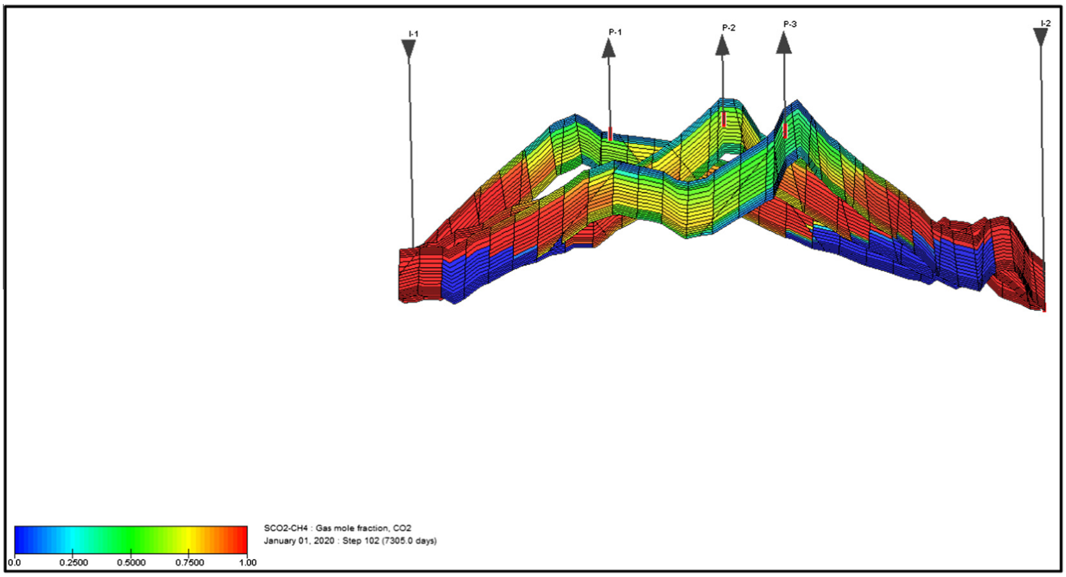


**Figure 15** Reservoir heterogeneity and $CO_2$ sweep efficiency.

favourable for $CO_2$ injection and allowed a greater amount of $CO_2$ to be injected. On the other hand, it will cause early breakthrough and detrimentally effects enhanced gas recovery.

Next we presented some results for the second case scenario, when $CO_2$ injection commenced after 5 years of gas production under normal production conditions. The simulation indicated that the high rate and early stage of $CO_2$ injection had the highest methane production and $CO_2$ storage at the same time it had the highest $CO_2$ production. Time appeared to have a significant impact on the planned strategies. The high rate and late stage of $CO_2$ injection appeared to be near the optimum strategy, because the higher natural gas production rate achieved within less time compared to the base-case and less time of $CO_2$ injection would have less costs of $CO_2$ compared to the first case scenario.

In addition, the second case scenario came as the second best $CO_2$ storage and it had lower $CO_2$ production compared to $CO_2$ production under the first case scenario. But this case can only be considered when the project is proposed for enhanced gas recovery because it has the highest $CO_2$ emissions due to late injection and releasing the production into the atmosphere before the commencement of $CO_2$ injection. Economically, this will affect the project when carbon tax is taken into account. As a result of comparisons between the case scenarios, high rate and early stage of $CO_2$ injection is the optimum and this case can be vital especially when the project is planned for a sequestration.

## 7. Economics

Calculations carried out using the model shown in the previous section for base natural gas recovery combined with $CO_2$ sequestration in a high $CO_2$ gas reservoir (9%) had shown favourable economy in terms of gas recovery and Carbon Credit.

Base recovery of methane with no enhanced mechanisms totalled for about (2476 million lb-mole) recovery with $CO_2$ vented totalled around (247 million lb-mole) (see Fig. 2). Under the optimum case, using $CO_2$-EGR, methane and CO2 recovery were around (2778 million lb-mole) and (526 million lb-mole), respectively, with $CO_2$ injection of (1402 million lb-mole) (see Figs. 4 and 10). For this case, estimation of the total additional $CO_2$ requirement for the injection was (875 million lb-mole). The additional $CO_2$ requirement at the commencement of injection was high, and then started to decline after $CO_2$ breakthrough. This additional $CO_2$ was purchased from a gas fired power plant, the cost and carbon credit adjustment was taken care of in the model.

In terms of cost, some capital expenditures associated with drilling, completion and equipment have been extracted based upon recent published data [1]. The costs originally were produced by Joint Association Survey (JAS) and recently been updated and published by Advanced Resource International (ARI). In general these costs had initially been calculated with the consideration of a fixed cost constant for site preparation and other fixed cost items and a variable cost that are changed with increases exponentially with depth (Table 6).

All costs associated with injection wells were taken into account during the cost preparation of CCS. Such as;

- Capital cost of site screening and evaluation.
- Capital cost of injection well equipment.
- Capital cost for drilling.
- Normal daily operating expenses.
- Surface maintenance.
- Subsurface maintenance.
- Consumable costs.

Normal cash flow was used as economic criterion to demonstrate a comparison between the base-case and the optimum case. In addition, economic evaluation for $CO_2$-EGR and storage was also assessed where the concepts of carbon tax and carbon credit were implemented based on the fiscal and economic assumptions outlined in Table 7.

A simple look at the economics of a base-case scenario, estimation of total cash flow was about 841 million US$. Paid carbon tax for the vented $CO_2$ was estimated at 47 million US$ as additional cost of $CO_2$ where carbon tax was considered. It was estimated to be of 808 million US$ as final cash flow for the project as shown in Fig. 16.

Under the optimum case, the project had an estimated cash flow about 656 million US$. An additional cost due to released $CO_2$ during the process of CCS was estimated around 54 million US$ as a carbon tax. Received price because of storage of the injected $CO_2$ totalled 278 million US$ as carbon credits. Total additional source of revenue for the project is estimated with a value of 224 million US$ as a net carbon credit. The final cumulative cash flow with consideration of net carbon credit was 224 million US$ (Fig. 17).

However the economic feasibility was most sensitive to wellhead natural gas price, carbon dioxide (separation, transportation and injection) costs, the ratio of carbon dioxide injected to incremental methane produced seemed to be favourable in the cases presented in this paper. The results presented in this paper suggest that EGR is economically feasible at carbon dioxide separation and capture on side or nearby quality $CO_2$ supply. Although the analysis is based on a particular gas field, the approach is general and can be applied to other gas fields. This economic analysis, along with the reservoir simulation and the laboratory studies demonstrate the technical feasibility of EGR. The base reservoir model used in this study was based on a known field in the North West Shelf. It was composed of sandstone which had homogeneous layer-cake geology and contained natural gas at a depth of 3650 m. Reservoir core samples were studied experimentally to accurately estimate the general petro-physical characteristics of the reservoir. The physical properties for each one of the tested cores were used as the base assignment to represent the geological model. The reservoir properties were then allocated throughout the reservoir simulation based on the interpretations of each pore plug. The gas reservoir model was created and controlled by variousness of cells distributions in terms of width, length and thickness.

The dimensions of the geological model, in the $X$-grid 17 grid-blocks were used and 22 grid-blocks were used in the $Y$ direction. The divisions in the $Z$ directions vary by layers, with 4, 3, 6 and 5 grid-blocks were formed to represent layers L1, L2, L3 and L4, respectively. The parameter values are distributed in such a way, for closeness to reality.

Starting from the upper part of the geological model, thickness of the first layer was 50 m, and it had a value of 0.04 porosity, 0.05 for critical gas saturation and 0.120 for critical water saturation. The permeability values distributed as 6, 6 and 4 md for $x$, $y$ and $x$ directions, respectively. For the second layer from the top of the reservoir, it had a thickness of 70 m. Porosity, critical gas and water saturation values for the existence thickness were determined as 0.17, 0.03 and 0.175, respectively. In addition, permeability values for this layer

**Table 6** Wells capital expenditures.

| Inputs | Equations | Fixed cost constant | |
|---|---|---|---|
| | | $a_1$ | $a_2$ |
| Well D and C costs | $y = a_0 \times D^{a1}$ | 2.7405 | 1.3665 |
| Production well equipping costs | $y = a_0 + a_1 D$ | 81403 | 7.033 |

**Table 7** Economic assumptions.

| Economic assumptions | |
|---|---|
| Methane wellhead price | 69 $/tonne |
| Carbon credit | 25 $/tonne |
| Carbon tax | 23 $/tonne |
| Energy penalty | 20% |
| $CO_2$ capture | 35 $/tonne |
| $CO_2$ transport | 13 $/tonne |
| $CO_2$ injection | 7 $/tonne |
| $CO_2$ separation | 5 $/tonne |
| Income tax | 30% |
| Royalty | 10% |

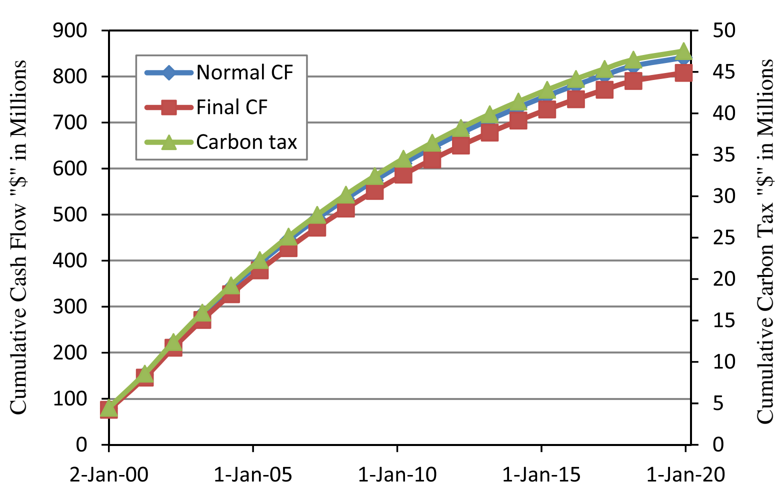


**Figure 16** Cash flow under the base-case with consideration of carbon tax.

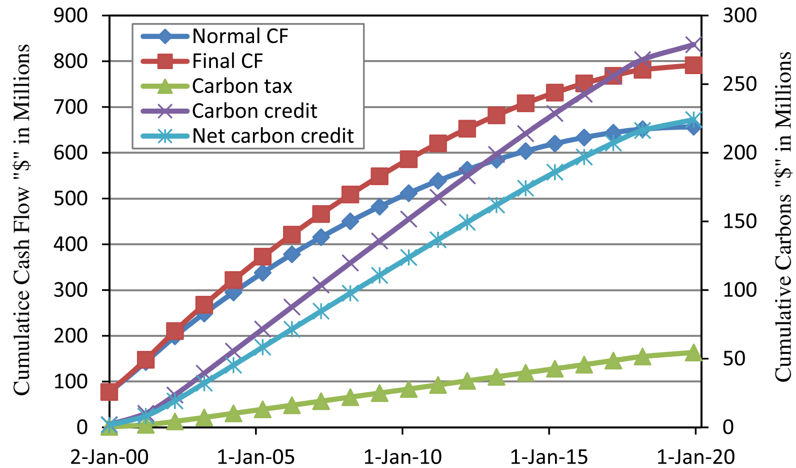


**Figure 17** Cash flow for the optimum-case with consideration of net carbon credit.

were distributed as 390, 390 and 370 md for *x*, *y* and *z* respectively. The third layer of the reservoir model was organized as porosity of 0.14, gas critical saturation with a value of 0.04 and 0.145 for critical water saturation with a thickness of 120 m. The bottom layer also demonstrated that EGR using own $CO_2$ could be feasible and that a field pilot study of the process should be undertaken to test the concept further. This study also demonstrated the use of additional $CO_2$ from industrial sources within reasonable range can add a value in terms of improved gas production plus extra earning from carbon credit.

## 8. Conclusion

Simulations of the process of $CO_2$, injection, into a natural gas reservoir carried out and confirmed the potentiality of $CO_2$ injection as a way to sequester carbon dioxide while enhancing methane recovery. Properties of natural gas and $CO_2$ are favourable for re-pressurization without extensive mixing over the estimated time periods. According to the simulation results, a comparison between the case scenarios suggested that the higher rates of $CO_2$ injection a significant improvement in cumulative natural gas recovery is achieved simultaneously large amount of $CO_2$ storage. Even though, the process of $CO_2$-EGR is technically and economically favourable, while if future carbon markets involve effective payment for $CO_2$ storage compared to carbon tax for $CO_2$ emissions the process will be more attractive.

## Acknowledgements

The authors would like to acknowledge the use of Roxar (Tempest) software in this research. The first author would also like to thank (CIPRS) for sponsoring his Ph.D course at Curtin University.

## Reference

[1] Advanced Resources International, Ten Basin-Oriented $CO_2$-EOR Assessments Examine Strategies for Increasing Domestic Oil Production. U.S. Department of Energy. <http://www.fe.doe.gov/programs/oilgas/eor/Ten_Basin-Oriented_CO2-EOR_Assessments.html>, 2006 (accessed 5.01.11).

[2] M. Algharaib, N. Abu Al-Soof, 2008. Economical modelling of $CO_2$ capturing and storage project. SPE paper 120815, presented at SPE Saudi Arabia Section Technical Symposium held in Alknobar, Saudi Arabia.

[3] A. Al-Hashami, S. Ren, B. Tohidi, 2005. $CO_2$ injection for enhanced gas recovery and geo-storage: Reservoir simulation and economics. SPE paper 94129, presented at the SPE Europe/EAGE Annual Conference held in Madrid, Spain.

[4] T. Clemens, K. Wit, 2002. $CO_2$ enhanced gas recovery studies for an example gas reservoir. SPE paper 77348, presented at SPE Annual Technical Conference and Exhibition held in San Antonio, Texas.

[5] O. Curtis, Carbon sequestration in natural gas reservoir: Enhanced gas recovery and natural gas storage. Conference: TOUGH Symposium 2003, Berkeley, CA (US), 05/12/2003–05/14/2003; Ernest Orlando Lawrence Berkeley National Laboratory, Berkeley, CA (US). DOE Scientific and Technical Information <http://www.osti.gov/bridge/product.biblio.jsp?osti_id=813580>, 2003 (accessed 12.12.10).

[6] J. David, Economic evaluation of leading technology options of sequestration of carbon dioxide. Msc diss., Massachusetts Institute of Technology. <http://sequestration.mit.edu/pdf/JeremyDavid_thesis.pdf>, 2000 (accessed 28.11.11).

[7] B. Feather, R. Archer, 2010. Enhance natural gas recovery by carbon dioxide injection for storage purposes. 17th Australia Fluid Mechanics Conference held in Auckland, New Zealand.

[8] A. Gaspar, G. Lima, S. Suslick, 2005. $CO_2$ capture and storage in mature oil reservoir: physical description, EOR and economic valuation of a case of a Brazilian mature field. SPE paper 94181, presented at SPE Europe/EAGE Annual Conference held in Madrid, Spain.

[9] C. Hussen, R. Amin, G. Madden, B. Evans, Reservoir simulation for enhanced gas recovery: an economic evaluation, J. Nat. Gas Sci. Eng. 5 (2012) (2012) 42–50.

[10] International Energy Agency, $CO_2$ Capture & Storage Energy. Technology Systems Analysis Programme (IEA-ETSAP). <http://www.iea-etsap.org/web/E-TechDS/PDF/E14_%20CCS%20draft%20oct2010_%20GS-gc_OK.pdf>, 2010 (accessed 5.04.11).

[11] P.R. Knox, S.D. Hovorka, C.M. Oldenburg, Potential new uses for old gas fields: sequestration of carbon dioxide: Gulf Coast Association of Geological Societies Transactions, 52, 563–571. GCCC Digital Publication Series #02-02. <http://

www.beg.utexas.edu/gccc/forum/codexdownloadpdf.php?ID = 7 >, 2002 (accessed 16.01.11).

[12] D. Mamora, G. Seo, 2002 (29 September-2 October). Enhanced gas recovery by carbon dioxide sequestration in depleted gas reservoir. SPE paper 77347, presented at the SPE Annual Technical Conference and Exhibition held in San Antonio, Texas.

[13] B. Meer, Carbon dioxide storage in natural gas reservoirs, Oil Gas Sci. Technol. 60 (3) (2005) 527–536.

[14] D. Nguyen, 2003. Carbon dioxide geological sequestration: technical and economic review. SPE paper 81199, presented at the SPE/EPA/DOE Exploration and Production Environmental Conference held in San Antonio, Texas, USA.

[15] D. Nguyen, W. Allinson, 2002. The economics of $CO_2$ capture and geological storage. SPE paper 77810, presented at the SPE Asia Pacific Oil and Gas Conference and Exhibition held in Melbourne, Australia.

[16] C. Oldenburg, S. Benson, 2002. $CO_2$ injection for enhanced gas production and carbon sequestration. SPE paper 74367, presented at the SPE International Petroleum Conference and Exhibition in Mexico held in Villahemosa.

[17] C. Oldenburg, K. Pruess, S. Benson, Process modelling of $CO_2$ injection into natural gas reservoirs for carbon sequestration and enhanced gas recovery. Earth Science Division 15, 293–298. Energy & Fuel, < http://pubs.acs.org/doi/abs/10.1021/ef000247h >, 2001 (accessed 16.07.10).

[18] C. Oldenburg, S. Stevens, S. Benson, Economic feasibility of carbon sequestration with enhanced gas recovery (CSEGR). Earth Sciences Division 29 (9–10), 1413–1422. Science Direct < http://www.sciencedirect.com/ >, 2004 (accessed 5.08.08).

[19] O. Ozkilic, F. Gumrah, Simulating $CO_2$ sequestration in a depleted gas reservoir. Taylor & Francis Group. Energy Sources, Part A, Volume 31, Issue 13. < http://www.tandfonline.com/doi/abs/10.1080/15567030801952235 >, 2009 (accessed 16.07.11).

[20] G. Seo, D. Mamora, Experimental and simulation studies of sequestration of supercritical carbon dioxide in depleted natural gas reservoirs, J. Energy Res. Technol. 127 (1) (2005).

[21] J. Willetts, D. Mason, L. Guerrera, P. Ryles, Legendre: maturation of a marginal offshore oil discovery to development project, Australian Petroleum Production and Exploration Association (APEA) Journal 39 (1999) 504–522.